ISSN 1995-0802, Lobachevskii Journal of Mathematics, 2024, Vol. 45, No. 4, pp. 1738–1747. © Pleiades Publishing, Ltd., 2024.

Numerical Modeling of Natural and Mixed Convection in a Confined Space

N. S. Sayidova*

(Submitted by A. V. Lapin)

Bukhara State University, Bukhara, 200100 Uzbekistan

Received February 8, 2024; revised February 29, 2024; accepted March 10, 2024

Abstract—To solve the problem, a numerical method and an effective algorithm were proposed, which made it possible to study heat and mass transfer processes in a confined plane-parallel and axisymmetric space of a complex configuration in a wide range of initial parameters both in a frozen flow regime and for chemical equilibrium between components. To describe the flow under consideration, a system of equations was used, derived from the Navier–Stokes equations for compressible gas. The original system of equations was written relative to the stream function ψ of vorticity ω in dimensionless form in a Cartesian coordinate frame under the condition of axial symmetry. The processes of mixing and transfer of gases in a closed region of complex geometry, characteristic of the structures of gas-phase reactors, were studied under conditions of interaction of free and forced convection, considering conjugate heat transfer. It was revealed that at certain values of the flow rate of the injected gas and the geometric dimensions of the calculation domain, the formation of the main one-vortex and twin-vortex flow patterns is possible.

DOI: 10.1134/S1995080224601486

Keywords and phrases: *mathematical model, axisymmetric, energy equation, velocity, temperature, cylindrical coordinate system.*

1. INTRODUCTION

The study of processes of free and mixed convective flows, considering heat and mass transfer, plays an important role in the development of science and technology. Research in this area is stimulated by the needs that emerge in power engineering, thermal power engineering, and chemical technology apparatus. The development of aviation, gas-phase reactors, nuclear energy, laser, rocket and space technology put forward new statements of problems of free and mixed convective flows.

The problem of numerical modeling of free and forced convective flows of reacting gas mixtures includes issues related to the mathematical modeling of flows with heat transfer and diffusion and solution methods.Thermal power devices and installations are designed based on the calculation of non-stationary convective heat and mass transfer. For example, non-stationary convection processes of heat exchange and convection occur in steam and hot water boilers, drying manifolds, radiators, and convectors of heat supply systems, and many other heat and mass transfer devices.

Numerous publications are devoted to the study of free and mixed convection in such devices [1–18].

In particular, in [19], the formulation and solution to the problem of studying unsteady fluid flow and heat transfer during free convection in a limited volume of a cylinder are presented. The system of differential equations for the transfer of momentum, energy, and continuity of fluid flow in partial derivatives is written in a cylindrical coordinate frame and in a conservative form. The Navier–Stokes equations of motion are written in the Boussinesq approximation. An algorithm was developed for the numerical implementation of solving partial differential equations for non-stationary convective heat and mass transfer using the finite difference method. Finite difference analogues of differential equations in

*E-mail: n.s.saidova@buxdu.uz

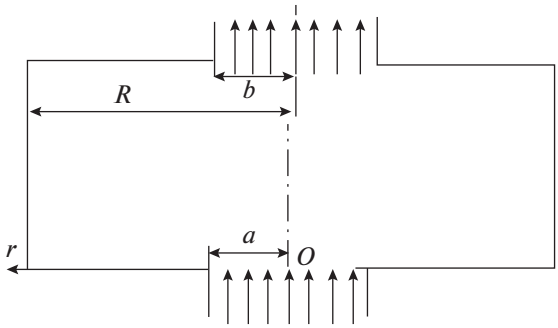

Fig. 1. Flow picture.

a conservative form were obtained. Calculated isolines are presented for the stream and vortex velocity functions for different values of dimensionless time [20]. Based on the calculation results, the occurrence of secondary flows and circulation of fluid movement inside a limited volume of a cylinder in the presence of a heat source was analyzed. Based on the calculation results, a stable region with intense fluid movement with flow stabilization was determined. A comparison of the results of numerical simulation with the data of physical experiments for the same types of flow is presented.

In [21], the stationary problem of forced convection in a rectangular region with arbitrarily located obstacles inside the region with inlet and outlet openings is considered. In the mathematical modeling of the problem under consideration, the Euler equation for an ideal incompressible fluid was used. A software package was developed; the numerical procedure is based on the SIMPLE algorithm. To increase the accuracy and achieve unconditional stability of the numerical integration method, and to save PC resources, the algorithm was modified taking into account the reality of the process. The disadvantage of mathematical modeling is the consideration of the problem as a model of an ideal incompressible fluid, which greatly narrows the scope of applicability [22, 23].

The study [24–26], simulated mixed convection turbulence in enclosed spaces filled with air. Numerically using Standard $k-e$, RNG $k-e$, and RSM turbulence models for various Richardson numbers. The governing equations were solved for small reminders using finite volume method.

In article [27], a simplified model of mixed convection in a limited space has been developed by approximating the solution of the basic equations by small-mode Fourier series and Chebyshev polynomials. The bifurcation structure of the simplified model, depending on two main parameters of the system: Re and Ar, has been numerically studied. Re is chosen as the bifurcation parameter.

The above brief review of the main literature sources shows that currently there is a large number of publications devoted to the study of motion under conditions of conjugate heat and mass transfer. However, there are still not enough publications that consider the simultaneous influence of factors using the limiting form of the complete system of Navier–Stokes equations for asymptotically small values of the hydrostatic compressibility parameter, the so-called model of essentially subsonic flows in the presence of significant changes in density, flow in a closed (limited) volume. Some issues require further research.

2. STATEMENT OF THE PROBLEM

We consider an isothermal gas jet flowing from a flat slot of a height of $2a$ into a rectangular region, propagating in it, and flowing out of a slot of a height of $2b$. In this case, the x axis is directed along the axis of the jet, which allows us to consider the problem in plan as axisymmetric, limiting ourselves to considering only half of the flow region: between the symmetry plane and the solid boundary. The flow pattern is shown in Fig. 1.

We write the basic equations through the stream ψ and vorticity ω functions in dimensionless form in a cylindrical coordinate frame under the condition of axial symmetry, which have the following form [28, 29]

$$\frac{\partial(\rho u\omega)}{\partial r}+\frac{\partial(\rho\vartheta\omega)}{\partial x}=\frac{\partial}{\partial r}\left(\mu\frac{\partial\omega}{\partial r}\right)+\frac{\partial}{\partial x}\left(\mu\frac{\partial\omega}{\partial x}\right)+\frac{\partial\rho}{\partial x}\frac{\partial}{\partial r}\left(\frac{u^2+\vartheta^2}{2}\right)-\frac{\partial\rho}{\partial r}\frac{\partial}{\partial x}\left(\frac{u^2+\vartheta^2}{2}\right)$$

$$+\frac{\partial\mu}{\partial r}\left[2\frac{\partial^2 u}{\partial r\,\partial x}+\frac{\partial^2\vartheta}{\partial r^2}+\frac{\partial^2\vartheta}{\partial x^2}\right]-\frac{\partial\mu}{\partial x}\left[2\frac{\partial^2\vartheta}{\partial r\,\partial x}+\frac{\partial^2 u}{\partial r^2}+\frac{\partial^2 u}{\partial x^2}\right]$$
$$+\left(\frac{\partial^2\mu}{\partial r^2}-\frac{\partial^2\mu}{\partial x^2}\right)\left(\frac{\partial u}{\partial x}+\frac{\partial\vartheta}{\partial x}\right)+2\,\frac{\partial^2\mu}{\partial r\partial x}\left(\frac{\partial\vartheta}{\partial x}-\frac{\partial u}{\partial r}\right), \tag{1}$$

$$\frac{\partial}{\partial r}\left(\frac{1}{\rho}\,\frac{\partial\psi}{\partial r}\right)+\frac{\partial}{\partial x}\left(\frac{1}{\rho}\,\frac{\partial\psi}{\partial x}\right)=-\omega, \tag{2}$$

$$\frac{\partial}{\partial r}(\rho u h)+\frac{\partial}{\partial x}(\rho\,\vartheta h)=\frac{1}{\mathrm{Pr}}\frac{1}{\mathrm{Re}}\left[\frac{\partial}{\partial r}\left(\lambda\frac{\partial h}{\partial r}\right)+\frac{\partial}{\partial x}\left(\lambda\frac{\partial h}{\partial x}\right)\right]. \tag{3}$$

The above task, i.e., system of equations (1)–(2) is solved under the following boundary conditions

$$\begin{aligned}
&x=0:\begin{cases}u=u_1, \quad v=0, \quad \text{when} \quad 0\le r<\alpha,\\ u=0, \quad v=0, \quad \text{when} \quad 0\le r<R,\end{cases}\\
&0<x<l: \quad u=0, \quad v=0, \quad \text{when} \quad r=R,\\
&x=l:\begin{cases}\dfrac{\partial u}{\partial x}=0, \quad \dfrac{\partial v}{\partial x}=0, \quad \text{when} \quad 0\le r<b,\\ u=0, \quad v=0, \quad \text{when} \quad b\le r<R,\end{cases}\\
&0<x<l:\frac{\partial u}{\partial x}=0, \quad v=0, \quad \text{when} \quad r=0.
\end{aligned} \tag{4}$$

The system of equations (1) and (2) with boundary conditions (4) for the stream function and vortex is written on a solid boundary in the following form

$$\psi_{CT}=0, \quad \left.\frac{\partial\psi}{\partial s}\right|_{CT}=0. \tag{5}$$

Since both of these conditions are specified only for the stream function, and not for the vortex, when numerically solving finite-difference approximations of these equations, the problem of determining the missing boundary conditions arises. One way to solve this problem is to expand the stream function into a series near the boundary. As an example, consider a solid boundary and write the expansion of $\psi_{i,1}$ into a Taylor series in the vicinity of point $(i,0)$ [30]:

$$\psi_{i,1}=\psi_{i,0}+\left.\frac{\partial\psi}{\partial x}\right|_{i,0}\Delta x+\frac{1}{2!}\left.\frac{\partial^2\psi}{\partial x^2}\right|_{i,0}\Delta x^2+\frac{1}{3!}\left.\frac{\partial^3\psi}{\partial x^3}\right|_{i,0}\Delta x^3+\ldots \quad . \tag{6}$$

If in expansion (6) we discard terms higher than the second order in Δx, considering that

$$\left.\frac{\partial\psi}{\partial x}\right|_{i,0}=r\rho\,u|_{i,0}=0$$

due to the adhesion condition,

$$\left.\frac{\partial^2\psi}{\partial x^2}\right|_{i,0}=\left.\frac{\partial(r\rho)}{\partial x}u\right|_{i,0}+r\rho\left.\frac{\partial u}{\partial x}\right|_{i,0}=r\rho\left.\frac{\partial u}{\partial x}\right|_{i,0},$$

and, in addition, $\omega=\frac{\partial\vartheta}{\partial r}-\frac{\partial u}{\partial x}$. Since $\vartheta=\mathrm{const}$ ($\vartheta=0$) along the wall, then $(\partial\vartheta\,/\,\partial r)|_{i,0}=0$. Therefore, $(\partial u\,/\,\partial x)|_{i,0}=-\omega_{i,0}$. Substituting these expressions into (6) and resolving with respect to $\omega_{i,0}$, we obtain

$$\omega_{i,0}=-\frac{2}{r_i\rho_{i,0}}\frac{\psi_{i,1}-\psi_{i,0}}{\Delta x^2}+O(\Delta x). \tag{7}$$

Thus, regardless of the orientation and the value of Ψ on the boundary, we can write

$$\omega_0=-\frac{2}{r_0\rho_0}\,\frac{\psi_1-\psi_0}{\Delta n^2}+0(\Delta n), \tag{8}$$

where Δn is the distance along the normal to the wall from the nearest wall of nodal point 1 to its projection O onto the wall, r_0, ρ_0 are the radius and density on a solid surface.

In the practical use of this formula, it is assumed that the boundary conditions (8) are satisfied. This leads to a simple relation connecting the vortex at the boundary with the stream function at the nearest boundary of the grid node

$$\omega_0 = -\frac{2}{r_0\rho_0}\frac{\psi_1}{\Delta n^2}. \tag{9}$$

In fact, when using formula (9), the no-slip boundary condition (5) is satisfied indirectly, i.e., on a solid wall there is a certain sliding velocity corresponding to the order of accuracy of the approximation of the derivative of the stream function [31]. In this case, the vortex at the boundary, in accordance with formula (8), is approximated with an accuracy of $O(\Delta n)$.

The boundary conditions on the axis (plane) of symmetry, on the input and output boundaries of the flow, were formulated as follows.

Let the axis of symmetry be the x axis of the Cartesian coordinate system. For the velocity components on the axis of symmetry the following conditions are set

$$\vartheta = 0, \quad \frac{\partial u}{\partial r} = 0. \tag{10}$$

The value of vorticity on the axis of symmetry is determined by the following relation

$$\omega = \frac{\partial \vartheta}{\partial r} - \frac{\partial u}{\partial x} = \Delta\psi, \tag{11}$$

which is written considering (10).

Velocity profiles are specified for the incoming flow, and the values of the stream function and vorticity are calculated based on the specified profiles. At the outlet, the distribution of these quantities is unknown, so the streamlines are assumed to be parallel to the axis, and the values of all variables are assumed to be constant along the streamline. At the outlet section, soft conditions were set for all the necessary parameters.

3. SOLUTION METHOD

Modeling physical processes [32, 33] is complex and to verify the adequacy of the model it is necessary to carry out numerical experiments [32], and also it is necessary to compare the results obtained with natural experiments or data obtained by other authors. In a similar way, we will solve the problem using numerical methods. For the Cartesian (and subsequently, for the cylindrical) coordinate frame, we introduce a non-uniform grid: r_i $(i = 1, 2, ..., N_r)$, x_i $(J = 1, 2, ..., N_x)$ with step along the r $(h_r)_i = r_i - r_{i-1}$, which depends on the number i of node r_i, and with a step along the axis x $(h_x)_j = x_j - x_{j-1}$ which depends on the number j of node x_j. When constructing a finite-difference approximation, a scheme with upstream differences, also called a scheme with donor cells, is widely used [4]. On each side of the node point of the spatial grid, some average velocities are found at the cell boundaries. The sign of these velocities determines from which grid node the values of the sought-for function F should be taken to write the upstream differences. In the one-dimensional case, we obtain

$$\omega = \frac{\partial \vartheta}{\partial r} - \frac{\partial u}{\partial x} = \Delta\psi, \tag{12}$$

where $u_R = \frac{1}{2}(u_{i+1} + u_i)$; $u_L = \frac{1}{2}(u_i + u_{i-1})$ is some transferable quantity.

The values of F are taken as follows [10]

$$F_R = \begin{cases} F_i, & u_R > 0, \\ F_{i+1}, & u_R < 0, \end{cases} \qquad F_L = \begin{cases} F_{i-1}, & u_L > 0, \\ F_i, & u_R < 0. \end{cases} \tag{13}$$

In the case of a non-uniform grid, the finite-difference approximation of the second derivative has the form

$$\frac{\partial^2 F}{\partial r^2} = \frac{2}{r_{i+1} - r_{i-1}}\left(\frac{F_{i+1}}{r_{i+1}}\frac{-F_i}{-r_i} - \frac{F_i}{r_i}\frac{-F_{i-1}}{-r_{i-1}}\right). \tag{14}$$

Since the main numerical results were obtained for a cylindrical coordinate frame, as an exception, we present the finite-difference form of the equations in a cylindrical coordinate frame. The transition to the form for the Cartesian coordinate frame, according to the given equations, is not difficult.

Since the vortex transfer equation (1), the energy transfer equation (3), and the continuity equations of the ith component (2) belong to the same type, they can be written in a generalized form

$$\frac{\partial(\rho uF)}{\partial r}+\frac{\partial(\rho\vartheta F)}{\partial x}=\frac{1}{\sqrt{Cr}}\left[\frac{1}{r}\frac{\partial}{\partial r}\left(rA_2\frac{\partial F}{\partial r}\right)+\frac{\partial}{\partial x}\left(A_2\frac{\partial F}{\partial x}\right)\right]-A_1F+A_3. \tag{15}$$

Thus, in the case of the vortex transfer equation, we assume

$$F=\omega;\quad A_1=\frac{1}{\sqrt{Gr}}\frac{\mu}{r^2};\quad A_2=\mu;$$

$$A_3=\frac{\partial\rho}{\partial r}\left[\frac{1}{\varepsilon_\rho}-\frac{\partial}{\partial x}\left(\frac{u^2+\vartheta^2}{2}\right)\right]+\frac{\partial\rho}{\partial x}\frac{\partial}{\partial r}\left(\frac{u^2+\vartheta^2}{2}\right)$$
$$+\frac{1}{\sqrt{Gr}}\left\{\frac{\partial\mu}{\partial r}\left[\frac{\partial^2u}{\partial r\partial x}+\frac{1}{r}\frac{\partial u}{\partial x}+\frac{1}{r}\frac{\partial}{\partial r}\left(r\frac{\partial\vartheta}{\partial r}\right)+2\frac{\partial^2\vartheta}{\partial x^2}\right]+\left(\frac{\partial^2\mu}{\partial r^2}-\frac{\partial^2\mu}{\partial x^2}\right)\right.$$
$$\left.\times\left(\frac{\partial u}{\partial x}+\frac{\partial\vartheta}{\partial r}\right)+2\frac{\partial^2\mu}{\partial r\partial x}\left(\frac{\partial\vartheta}{\partial x}-\frac{\partial u}{\partial r}\right)-\frac{\partial\mu}{\partial x}\left[2\frac{\partial}{\partial r}\left(\frac{1}{r}\frac{\partial(ru)}{\partial r}\right)+\frac{\partial^2u}{\partial x^2}+\frac{\partial^2\vartheta}{\partial r\partial x}\right]\right\}. \tag{16}$$

For the energy equation

$$F=h;\quad A_1=\frac{\rho u}{r};\quad A_2=\frac{\mu}{\mathrm{Pr}};$$

$$A_3=\frac{1}{\sqrt{Gr}}\left\{\frac{1}{r}\frac{\partial}{\partial r}\left[r\sum_{k=1}^{N_K}E_k\frac{\partial C_k}{\partial r}\right]+\frac{\partial}{\partial x}\left[\sum_{k=1}^{N_K}E_k\frac{\partial C_k}{\partial x}\right]\right\}, \tag{17}$$

where $E_k=\left(\frac{\mu}{Sc_K}-\frac{\mu}{\mathrm{Pr}}\right)h_k$.

It should be noted that two limiting cases of chemical interaction between components: frozen and equilibrium, are considered in this study. The continuity equations of ith components (2) for a frozen flow are simplified, as the term expressing the mass rate of formation of the ith component is zero, i.e., w_i=0. Then, for the mass transfer equation of the kth component, we have

$$F=C_k;\quad A_1=\frac{\rho u}{r};\quad A_3=0;\quad A_2=\frac{\mu}{Sc_k}(k=1,2,...,N). \tag{18}$$

For the diffusion equation of the kth element

$$F=C_k^*,\quad k=1,2,...,N;\quad A_1=\frac{\rho u}{r};\quad A_2=\frac{\mu}{Sc^*}; \tag{19}$$

$$A_3=\frac{1}{\sqrt{Gr}}\left\{\frac{1}{r}\frac{\partial}{\partial r}\left[r\sum_{l=1}^{N_K}E_l\frac{\partial C_l}{\partial r}\right]+\frac{\partial}{\partial x}\left[\sum_{l=1}^{N_K}E_l\frac{\partial C_l}{\partial x}\right]\right\},$$

here $E_l=C_{kl}\left(\frac{\mu}{Sc_l}-\frac{\mu}{Sc^*}\right)$.

Let us write the generalized equation (15) in finite-difference form, considering the fact that the implicit method of alternating directions is used to solve it. According to the concept of the establishment method, a non-stationary term is added to the left-hand side of the equation. The convective terms of the equation are approximated using an upstream scheme, and the diffusion terms are approximated by central differences [10]. Thus, the finite-difference form of the generalized equation (15) has the following form

—in the first half step

$$\frac{F_{i,j}^{n+1/2}-F_{i,j}^{n}}{0,5\tau}+\left[\frac{(u_R-|u_R|)F_{i+1,j}^{n+1/2}+(u_R+|u_R|-u_L+|u_L|)F_{ij}^{n+1/2}-(u_L+|u_L|)F_{i-1.j}^{n+1/2}}{2(r_{i+1}-r_{i-1})}\right.$$

$$+\left[(\vartheta_R-|\vartheta_R|)F^n_{i,j+1}+(\vartheta_R+|\vartheta_R|-\vartheta_L+|\vartheta_L|)F^n_{i,j}-(\vartheta_L+|\vartheta_L|)F^n_{i,j-1}\right]/2(x_{j+1}-x_{j-1})$$
$$=\frac{1}{\sqrt{Gr}}\left\{\frac{1}{r_{i+1}-r_{i-1}}\left[\frac{(A_2)^n_{i,j}+(A_2)^n_{i+1,j}}{r_{i+1}-r_i}\left(F^{n+1/2}_{i+1,j}-F^{n+1/2}_{i,j}\right)\right.\right.$$
$$\left.-\frac{(A_2)^n_{i,j}+(A_2)^n_{i-1,j}}{r_i-r_{i-1}}\left(F^{n+1/2}_{i,j}-F^{n+1/2}_{i-1,j}\right)\right]+\frac{(A_2)^n_{i,j}}{r_i}\,\frac{F^{n+1/2}_{i+1,j}-F^{n+1/2}_{i-1,j}}{r_{i+1}-r_{i-1}}$$
$$+\frac{1}{x_{j+1}-x_{j-1}}\left[\frac{(A_2)^n_{i,j}+(A_2)^n_{i,j+1}}{x_{j+1}-x_j}\left(F^n_{i,j+1}-F^n_{i,j}\right)\right.$$
$$\left.\left.-\frac{(A_2)^n_{i,j}+(A_2)^n_{i,j-1}}{x_j-x_{j-1}}\left(F^n_{i,j}-F^n_{i,j-1}\right)\right]\right\}$$
$$-(A_1)^n_{i,j}F^{n+1/2}_{i,j}+(A_3)^n_{i,j}, \tag{20}$$

—in the second half step

$$\frac{F^{n+1}_{i,j}-F^{n+1/2}_{i,j}}{0,5\tau}+\left[\frac{(u_R-|u_R|)F^{n+1/2}_{i+1,j}+(u_R+|u_R|-u_L+|u_L|)F^{n+1/2}_{ij}-(u_L+|u_L|)F^{n+1/2}_{i-1.j}}{2(r_{i+1}-r_{i-1})}\right]$$
$$+\left[(\vartheta_R-|\vartheta_R|)F^{n+1}_{i,j+1}+(\vartheta_R+|\vartheta_R|-\vartheta_L+|\vartheta_L|)F^{n+1}_{i,j}-(\vartheta_L+|\vartheta_L|)F^{n+1}_{i,j-1}\right]/2(x_{j+1}-x_{j-1})$$
$$=\frac{1}{\sqrt{Gr}}\left\{\frac{1}{r_{i+1}-r_{i-1}}\left[\frac{(A_2)^n_{i,j}+(A_2)^n_{i+1,j}}{r_{i+1}-r_i}(F^{n+1/2}_{i+1,j}-F^{n+1/2}_{i,j})\right.\right.$$
$$\left.-\frac{(A_2)^n_{i,j}+(A_2)^n_{i-1,j}}{r_i-r_{i-1}}(F^{n+1/2}_{i,j}-F^{n+1/2}_{i-1,j})\right]+\frac{(A_2)^n_{i,j}}{r_i}\frac{F^{n+1/2}_{i+1,j}-F^{n+1/2}_{i-1,j}}{r_{i+1}-r_{i-1}}$$
$$+\frac{1}{x_{j+1}-x_{j-1}}\left[\frac{(A_2)^n_{i,j}+(A_2)^n_{i,j+1}}{x_{j+1}-x_j}(F^{n+1}_{i,j+1}-F^{n+1}_{i,j})\right.$$
$$\left.\left.-\frac{(A_2)^n_{i,j}+(A_2)^n_{i,j-1}}{x_j-x_{j-1}}(F^{n+1}_{i,j}-F^{n+1}_{i,j-1})\right]\right\}-(A_1)^n_{i,j}F^{n+1}_{i,j}+(A_3)^n_{i,j}, \tag{21}$$

where

$$u_R=\rho^n_{i+1,j}u^n_{i+1,j}+\rho^n_{i,j}u^n_{i,j},\quad u_L=\rho^n_{i,j}u^n_{i,j}+\rho^n_{i-1,j}u^n_{i-1,j},$$
$$\vartheta_R=\rho^n_{i,j+1}\vartheta^n_{i,j+1}+\rho^n_{i,j}\vartheta^n_{i,j},\quad \vartheta_L=\rho^{\,n}_{i,j}\vartheta^n_{i,j}+\rho^n_{i,j-1}\upsilon^n_{i,j-1},$$

here τ is the time step in accordance with the concept of the establishment method.

Let us proceed to discussing the calculation algorithm. As in the case of compiling a mathematical model, we will represent the flow region in terms of a cylindrical coordinate frame. In a flat statement, the axial section of the cylindrical region is replaced by a section that is located in the plane of gas motion and orthogonal to the solid walls.

The mesh is refined near all solid boundaries, and the step in these places is reduced by three times relative to the central zone. Thus, the area under consideration is covered with a regular grid. It can be noted that non-uniform coordinates are obtained on the Or and Ox, axis, this is especially useful when the gradients of the sought-for variables are significant. The time step τ is selected in accordance with the recommendations given in [1], where numerous methodological calculations were conducted to select the optimal time step. Below is an algorithm for solving the problem of free and mixed convective flows of a multi-component chemically reacting gas under conditions of conjugate heat and mass transfer.

The coordinates of the grid nodes are calculated in accordance with the procedure described above. The initial values ψ^n; ω^n; T^n; C^n_k, $k=1,2,...,N_k$ are set; From the given fields of the current function, temperature and concentration of components, one can determine the fields of projection of velocities, density, specific enthalpy, transfer coefficients, as well as local Prandtl and Schmidt numbers of the the kth component.

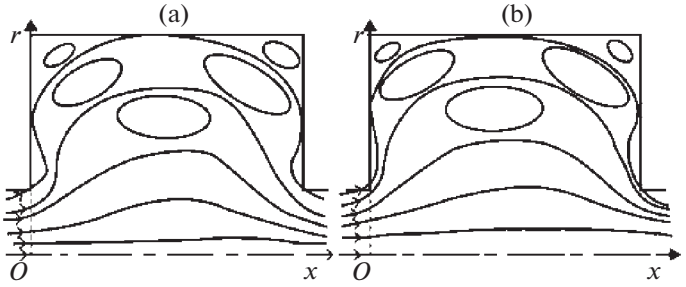

Fig. 2. Vortex field at velocities $\overline{u_1} = (a)$ 0.1 and (b) 0.5 m/s.

From equations (20) and (21) the vortex field $\omega_{i,j}^{n+1}$ is found by longitudinal transverse sweep. In this case, the values of the vortex at the boundary are taken from the previous iteration.

Calculation of the field of the stream function $\psi_{i,j}^{n+1}$ using formulas (20), (21) with known values of $\omega_{i,j}^{n+1}$ is carried out up to obtaining a stationary solution, i.e., the scheme includes an internal iterative loop for each time layer. The internal iterative loop is exited when the following condition is met

$$\max \left|\psi_{i,j}^{n+1,s+1} - \psi_{i,j}^{n+1,s}\right| < \varepsilon_1, \tag{22}$$

where $\varepsilon_1 = 10^{-3}$ is the accuracy of calculating the sought-for functions.

Using finite-difference analogues of the equations, the velocity projection fields u_{ij}^{n+1} and ϑ_{ij}^{n+1} are determined.

Using the resulting stream function field ψ_{ij}^{n+1}, the vortex values are calculated using formula (8) at the boundaries of the region for the next time step. When calculating the vortex on a circle, the procedure described above is applied.

Using the known value h_0^{n+1}, equations (20), (21) are solved and the specific enthalpy field h_{ij}^{n+1} is determined. From the known relationships [3] the temperature in the gas region is found. The distribution of temperature and concentration of the gas mixture makes it possible to determine the heat flow at the gas–solid interface.

The transition is made to the $(n+2)$th time layer, etc. The convergence of the iterative process is checked from the conditions

$$\max \left|\omega_{ij}^{n+1} - \omega_{ij}^{n}\right| < 10^{-5}, \quad \max \left|T_{ij}^{n+1} - T_{ij}^{n}\right| < 10^{-4} T_{ij}^{n+1}. \tag{23}$$

4. RESULTS

This algorithm is the result of detailed methodological studies that were conducted to improve the convergence and stability of calculations. According to the proposed algorithm, test calculations of gas flow in a rectangular area were performed. Based on the developed algorithm and solution method, calculations were performed for the following options of initial parameter values

$$\begin{aligned}
&1) \quad u_1 = \overline{u} u_0 = 0.1\,\text{m/s}, \quad \vartheta = 0\,\text{m/s}, \quad \rho = \text{const}, \quad T = 300\,\text{K},\\
&2) \quad u_1 = \overline{u} u_0 = 0.5\,\text{m/s}, \quad \vartheta = 0\,\text{m/s}, \quad T_1 = 500\,\text{K}, \quad T_2 = 300\,\text{K},\\
&4) \quad u_1 = \overline{u} u_0 = 0.5\,\text{m/s}, \quad \vartheta = 0\,\text{m/s}, \quad T_1 = 500\,\text{K}, \quad T_2 = 300\,\text{K}.
\end{aligned}$$

The main results of the calculations are presented in the form of graphs in Figs. 2 and 3. In Fig. 2, the shapes of the stream function obtained with the original option 1 are shown.

As follows from the figure, four stagnant zones have formed: in the upper corners and at the wall near the entrance and exit. Closed isolines are shown only in stagnation zone near a corner. The formation of a stagnation zone near the inlet and outlet is due to the attempt of the flow to form the flow pattern that

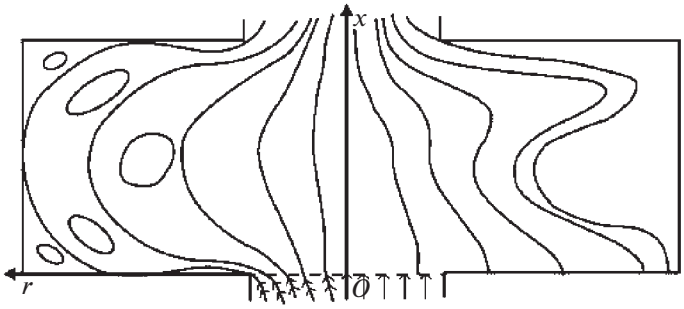

Fig. 3. Velocity and temperature vortex fields.

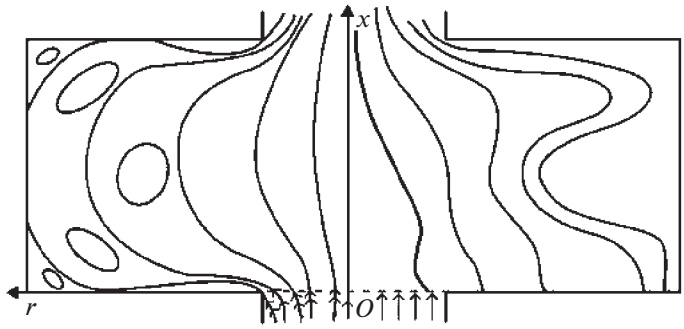

Fig. 4. Velocity and temperature vortex fields.

is most favorable from the point of view of reducing frictional resistance. In addition, three large eddies characteristic of secondary flows were observed.

Figure 3 shows the stream function isolines corresponding to option 2.

As follows from the figure, the zones of stagnation near a corner at $u_1 = 0.5$ m/s turned out to be smaller than at $u_1 = 0.1$ m/s. This can be explained by the fact that when the velocity value at the inlet increases due to the inertial force in a limited area, the flow is compressed and thereby the stagnant region is reduced or compacted, due to which the velocity field in the inlet and outlet sections is greater than for $u_1 = 0.1$ m/s, which clearly reflects the physics of the phenomenon.

Figure 3 shows the stream functions and temperature. It follows from the figure that inside a limited space, due to air preheating, stagnation areas in the corner and near-mouth zones are reduced. Moreover, the near-mouth stagnation zones become thinner and longer, although here the velocity of the inlet section is $u_1 = 0.1$ m/s. Figure 4 shows the field of the stream function and temperature at $u_1 = 0.5$ m/s. Here we can see graphs qualitatively similar to the previous ones. However, from the graph, we can say that the propagation of a jet of airflow in a confined space under gas heating almost covers the entire volume. Judging by the graphs, we can say that when the wall is heated, the mixing and distribution of airflow is much more effective than in the isothermal case.

5. CONCLUSIONS

A numerical method and an effective algorithm were proposed that make it possible to study heat and mass transfer processes in a confined plane-parallel and axisymmetric space of a complex configuration in a wide range of initial parameters both in a frozen flow regime and for chemical equilibrium between components. The complexity of the form of the calculation domain is due to the presence of a cylindrical surface in the plane-parallel region and the presence of a toroidal surface in the axisymmetric region.

The processes of mixing and transfer of gases in an enclosed region of complex geometry, characteristic of the structures of gas-phase reactors, were studied under conditions of interaction of free and forced convection, considering conjugate heat exchange. It was revealed that at certain values of the flow rate of the injected gas and geometric dimensions of the calculation domain, the formation of the main one-vortex and twin-vortex flow patterns is possible.

FUNDING

This work was supported by ongoing institutional funding. No additional grants to carry out or direct this particular research were obtained.

CONFLICT OF INTEREST

The author of this work declares that she has no conflicts of interest.

REFERENCES

1. I. J. Uwanta and E. Omokhuale, "Viscoelastic fluid flow in a fixed plane with heat and mass transfer," Res. J. Math. Stat. **4** (3), 63–69 (2012).
2. B. J. Gireesha, B. Mahanthesh, R. Gorla, and P. T. Manjunatha, "Thermal radiation and Hall effects on boundary layer flow past a non-isothermal stretching surface embedded in porous medium with non-uniform heat source/sink and fluid-particle suspension," Heat Mass Transfer **52**, 897–911 (2016).
3. B. J. Gireesha, B. Mahanthesh, R. Gorla, and P. T. Manjunatha, "Numerical solution for hydromagnetic boundary layer flow and heat transfer past a stretching surface embedded in non-Darcy porous medium with fluid-particle suspension," J. Niger. Math. Soc. **34**, 267–285 (2015).
4. M. A. Botchev and V. T. Zhukov, "Exponential Euler and backward Euler methods for nonlinear heat conduction problems," Lobachevskii J. Math. **44**, 10–19 (2023).
5. O. B. Feodoritova, N. D. Novikova, and V. T. Zhukov, "Development of numerical methodology for unsteady fluid solid thermal interaction in multicomponent flow simulation," Lobachevskii J. Math. **44**, 33–43 (2023).
6. P. Kiva, N. Grafeeva, and E. Mikhailova, "A machine learning approach to calculating the non-equilibrium diffusion coefficients in the state-to-state solution of the Navier–Stokes equations," Lobachevskii J. Math. **44**, 170–177 (2023).
7. A. K. Da Silva and L. Gosselin, "On the thermal performance of an internally finned three-dimensional cubic enclosure in natural convection," Int. J. Therm. Sci. **44**, 540–546 (2005).
8. A. Berdyshev, R. Aloev, Zh. Abdiramanov, and M. Ovlayeva, "An explicit implicit upwind difference splitting scheme in directions for a mixed boundary control problem for a two-dimensional symmetric t-hyperbolic system," Symmetry **15** (10) (2023). https://doi.org/10.3390/sym15101863
9. D. A. Koc, "A numerical scheme for time-fractional fourth-order reaction-diffusion model," J. Appl. Math. Comput. Mech. **22**, 540–546 (2023). https://doi.org/10.17512/jamcm.2023.2.02
10. G. Kuznetsov and M. Sheremet, "A numerical simulation of double-diffusive conjugate natural convection in an enclosure," Int. J. Therm. Sci. **50**, 1878–1886 (2011).
11. M. K. Chourasia and T. Goswami, "Three dimensional modeling on airflow, heat and mass transfer in partially impermeable enclosure containing agricultural produce during natural convective cooling," Energy Convers. Manage. **48**, 2136–2149 (2007).
12. A. Rautian and V. Vlasov, "Spectral analysis of the generators for semigroups associated with Volterra integro-differential equation," Lobachevskii J. Math. **44**, 926–935 (2023).
13. A. Rautian and V. Vlasov, "A spectral Sobolev problem for the biharmonic operator," Lobachevskii J. Math. **44**, 950–955 (2023).
14. V. Baranchuk and S. Pyatkov, "On some inverse problems of recovering sources in stationary convection-diffusion models," Lobachevskii J. Math. **44**, 1111–1118 (2023).
15. N. Ravshanov and T. Shafiev, "Nonlinear mathematical model for monitoring and predicting the process of transfer and diffusion of fine-dispersed aerosol particles in the atmosphere," J. Phys.: Conf. Ser. **1260**, 1–7 (2019).
16. N. Ravshanov, Z. Abdullaev, and T. Shafiyev, "Mathematical model and numerical algortm to study the process of aerosol particles distribution in the atmosphere," in *Proceedings of the International Conference on Information Science and Communications Technologies* (2019), pp. 1–7.
17. A. Lapin and R. Yanbarisov, "Numerical solution of a subdiffusion equation with variable order time fractional derivative and nonlinear diffusion coefficient," Lobachevskii J. Math. **44**, 2790–2803 (2023).
18. F. Muradov and D. Akhmedov, "Numerical modeling of atmospheric pollutants dispersion taking into account particles settling velocity," in *Proceedings of the International Conference on Information Science and Communications Technologies* (2019), pp. 1–5.
19. S. Bouzid, Y. Harnane, and A. Brima, "Characterization of turbulent natural and mixed convection in confined enclosures equipped with a heat source," Instrum. Mesure, Metrol. **17**, 63 (2018).
20. Z. Gao, Z. Liu, Y. Wei, C. Li, S. Wang, X. Qi, and W. Huang, "Numerical analysis on the influence of vortex motion in a reverse Stairmand cyclone separator by using LES model," Pet. Sci. **19**, 848–860 (2022).

21. S. Nabi, P. Grover, and C. Caulfield, "Adjoint-based optimization of displacement ventilation flow," Build. Environ. **124**, 342–356 (2017).
22. V. Zharov, I. Lipatov, and R. Selim, "Mathematical modeling of incompressible fluid flow in turbulent boundary layers," in *Proceedings of the International Scientific Conference on Architecture and Construction* (Springer Nature, Singapore, 2020), pp. 391–405.
23. M. Deville, *An Introduction to the Mechanics of Incompressible Fluids* (Springer Nature, Cham, 2022).
24. M. Safaei and M. Mohammadi, "Numerical modeling of turbulence mixed convection heat transfer in air filled enclosures by finite volume method," Int. J. Multiphys. **5**, 307–324 (2011).
25. M. Rahman, M. Alim, M. Mamun, M. Chowdhury, and A. Islam, "Numerical study of opposing mixed convection in a vented enclosure," ARPN J. Eng. Appl. Sci. **2** (2), 25–36 (2007).
26. K. Khanafer, A. Al-Amiri, and I. Pop, "Numerical simulation of unsteady mixed convection in a driven cavity using an externally excited sliding lid," Eur. J. Mech., B: Fluids **26**, 669–687 (2007).
27. G. Xin, W. Chow, and S. Liu, "Windows and routes to chaos in mixed convection in confined spaces," Chaos Solitons Fract. **15**, 543–558 (2003).
28. A. Filippov and V. Popov, "Using cylindrical and spherical symmetries in numerical simulations of quasi-infinite mechanical systems," Symmetry **14**, 1557 (2022).
29. A. Ryabokona and O. Tkachenkoa, "Mathematical model of intersecting cylindrical shells in Cartesian coordinates," in *CEUR Workshop Proceedings* (2021), pp. 119–126.
30. T. Jacquemin, S. Tomar, K. Agathos, S. Mohseni-Mofidi, and S. Bordas, "Taylor-series expansion based numerical methods: A primer, performance benchmarking and new approaches for problems with non-smooth solutions," Arch. Comput. Methods Eng. **27**, 1465–1513 (2020).
31. V. Polezhaev, A. Bune, N. Verezub, G. Glushko, and V. Gryaznov, *Mathematical Modeling of Convective Heat and Mass Transfer on the Basis of the Navier–Stokes Equations* (Nauka, Moscow, 1987) [in Russian].
32. I. Shadmanov and T. Shafiyev, "Mathematical modeling of the processes of combined heat and moisture transfer during storage and drying of raw cotton," E3S Web Conf. **431**, 01060 (2023).
33. T. Shafiev and Sh. Nazarov, "Studies of the influence of vegetation cover on the process of transfer and diffusion of harmful substances in the atmosphere," E3S Web Conf. **431**, 01059 (2023).
34. T. Shafiev, G. Shadmanova, G. Karimovam, and F. Muradov, "Nonlinear mathematical model and numerical algorithm for monitoring and predicting the concentration of harmful substances in the atmosphere," E3S Web of Conf. **264**, 01021 (2021).